

ARMY RESEARCH LABORATORY



A Fluorescence-Based Determination of Quantum Efficiency

by Scott Melis

ARL-CR-0726

December 2013

NOTICES

Disclaimers

The findings in this report are not to be construed as an official Department of the Army position unless so designated by other authorized documents.

Citation of manufacturer's or trade names does not constitute an official endorsement or approval of the use thereof.

Destroy this report when it is no longer needed. Do not return it to the originator.

Army Research Laboratory

Adelphi, MD 20783-1197

ARL-CR-0726

December 2013

A Fluorescence-Based Determination of Quantum Efficiency

Scott Melis

American Society for Engineering Education

1818 N Street, N. W., Suite 600

Washington, DC 20036-2479

REPORT DOCUMENTATION PAGE

Form Approved
OMB No. 0704-0188

Public reporting burden for this collection of information is estimated to average 1 hour per response, including the time for reviewing instructions, searching existing data sources, gathering and maintaining the data needed, and completing and reviewing the collection information. Send comments regarding this burden estimate or any other aspect of this collection of information, including suggestions for reducing the burden, to Department of Defense, Washington Headquarters Services, Directorate for Information Operations and Reports (0704-0188), 1215 Jefferson Davis Highway, Suite 1204, Arlington, VA 22202-4302. Respondents should be aware that notwithstanding any other provision of law, no person shall be subject to any penalty for failing to comply with a collection of information if it does not display a currently valid OMB control number.

PLEASE DO NOT RETURN YOUR FORM TO THE ABOVE ADDRESS.

1. REPORT DATE (DD-MM-YYYY) December 2013		2. REPORT TYPE Final		3. DATES COVERED (From - To) May to August 2013	
4. TITLE AND SUBTITLE A Fluorescence-Based Determination of Quantum Efficiency				5a. CONTRACT NUMBER W911NF-10-2-0076	
				5b. GRANT NUMBER	
				5c. PROGRAM ELEMENT NUMBER	
6. AUTHOR(S) Scott Melis				5d. PROJECT NUMBER SEAP-CQL	
				5e. TASK NUMBER	
				5f. WORK UNIT NUMBER	
7. PERFORMING ORGANIZATION NAME(S) AND ADDRESS(ES) U.S. Army Research Laboratory ATTN: RDRL-SEE-M 2800 Powder Mill Rd Adelphi MD 20783-1197				8. PERFORMING ORGANIZATION REPORT NUMBER ARL-CR-0726	
9. SPONSORING/MONITORING AGENCY NAME(S) AND ADDRESS(ES) U. S. Army Research Office Technology Integration and Outreach Office P. O. Box 12211 Research Triangle Park, NC 27709-2211				10. SPONSOR/MONITOR'S ACRONYM(S)	
				11. SPONSOR/MONITOR'S REPORT NUMBER(S)	
12. DISTRIBUTION/AVAILABILITY STATEMENT Approved for public release; distribution unlimited.					
13. SUPPLEMENTARY NOTES larry.d.merkle.civ@mail.mil					
14. ABSTRACT This work attempts to apply the method of determining quantum efficiency described by de Mello et al. in order to verify that it is accurate and can be used to measure unknown samples in the future. This method takes direct spectra of the fluorescence of a sample excited by an incoming excitation laser beam in an integrating sphere. Three scenarios are considered: a sphere with no sample inside such that only the laser light is scattered, a sphere with the sample inside but not in the direct path of the laser, and a sample inside and in the direct path of the laser. Samples of 1% ceramic neodymium (Nd): yttrium aluminum garnet (YAG) and 10% crystal ytterbium (Yb):YAG (chosen after the poor result achieved for Nd:YAG) were tested, since both are thought to have high quantum efficiencies of close to 1. In this experiment, the quantum efficiency values determined were 0.54 and 0.99, respectively. These results forced a consideration of all possible sources of error in this method; future work will be needed to determine if the technique is still viable.					
15. SUBJECT TERMS Quantum efficiency, fluorescence, Nd, Yb, YAG, integrating sphere					
16. SECURITY CLASSIFICATION OF:			17. LIMITATION OF ABSTRACT UU	18. NUMBER OF PAGES 24	19a. NAME OF RESPONSIBLE PERSON Larry D. Merkle
a. REPORT Unclassified	b. ABSTRACT Unclassified	c. THIS PAGE Unclassified			19b. TELEPHONE NUMBER (Include area code) (301) 394-0941

Contents

Lift of Figures	iv
List of Tables	iv
1. Background	1
2. Introduction	1
3. Equipment	1
4. Experiment	2
5. Results	3
6. Analysis	5
7. Retrial With 10% Yb:YAG	6
8. Conclusions	8
9. References	9
Appendix A. System Response Curves	11
Appendix B. Example of the Data Analysis	13
Appendix C. Transmission Spectra of Samples	15
Appendix D. Data for Reabsorption Determination for Yb:YAG	17
Distribution List	18

List of Figures

Figure 1. Diagram showing the three scenarios for the quantum efficiency measurement. (1) The sphere is empty. (2) The sample is in the sphere but out of the beam. (3) The sample is in the sphere and in the beam.....	3
Figure 2. This is the raw spectrum produced by the 1% Nd:YAG sample located directly in the beam. The out of the beam case produced a similar spectrum with smaller fluorescence values and a larger laser line.....	5
Figure 3. Raw spectrum produced by the 10% Yb:YAG sample located directly in the beam. The out of the beam case produced a similar spectrum with smaller fluorescence values and a larger laser line. The laser line for this scenario peaked at 9.5 on this scale and has been cut off for clarity of the fluorescence spectrum.	7
Figure A-1. Normalized system response curve generated for the aluminum holder in the integrating sphere in conjunction with the 2.2- μm InGaAs detector and the 1- μm blazed grating.	11
Figure A-2. Normalized system response curve obtained when the same method was applied to the coated sample holder in conjunction with the 2.2- μm InGaAs detector and the 1- μm blazed grating.....	12
Figure B-1. True fluorescence spectrum of 1% ceramic Nd:YAG.....	13
Figure B-2. Photon flux of 1% ceramic Nd:YAG.	14
Figure C-1. Transmission spectrum for the 1% ceramic Nd:YAG sample used in this experiment.....	15
Figure C-2. Transmission spectrum for the 10% Yb:YAG sample used in this experiment.....	16
Figure D-1. Photon flux scaled for the detection system for the powdered sample and the bulk sample measured directly in the spectrometer.....	17

List of Tables

Table 1. Values for L_e , L_o , L_i , F_o , and F_i using the 1% Nd:YAG sample.	5
Table 2. Values for L_e , L_o , L_i , F_o , and F_i using the 10% Yb:YAG sample.	7

1. Background

The quantum efficiency of a material is an important measurement in laser applications. It is defined as the percentage of incident photons that a material converts to fluorescence, with the energy of the unconverted photons being wasted as heat. A high quantum efficiency value would therefore allow the material to waste little energy when it is lased. This makes the material more useful as a laser for three reasons. First, there is no risk of overheating the laser material, since little energy is converted to heat. Heating it by too much could degrade the material or the beam quality, making the laser less effective at whatever tasks are required. Second, the lowered heating means that the laser is easier to construct and operate because it requires simpler cooling processes. Finally, a highly efficient laser material would require less power to operate, since the input power is more readily converted to light. With these goals in mind, a determination of whether or not a material possesses a high value of quantum efficiency is very necessary in laser applications and laser material research.

2. Introduction

The goal of this project was to interpret the method used by de Mello et al. (*1*) for calculating quantum efficiency and apply it to enable accurate measurements of bulk materials. Doing so would validate this method as well as create a setup that could be used to analyze future samples of unknown efficiency. To do this, a standard sample was needed to validate the technique. For this, a sample of 1% ceramic neodymium (Nd): yttrium aluminum garnet (YAG) was chosen. In addition, when the results with Nd:YAG proved to be incorrect, a sample of 10% ytterbium (Yb):YAG was also selected. Both samples were chosen due to their well-known and accepted high quantum efficiency values of close to 1.

3. Equipment

The following equipment was used:

- Spectra-Physics titanium sapphire laser
- Horiba Fluorolog 3 fluorescence spectrometer
 - With a nominally 2.6- μm indium gallium arsenide (InGaAs) detector and 1- μm blazed grating

- With a nominally 2.2- μm InGaAs detector and 1- μm blazed grating
 - Stanford Research Systems SR830 lock-in amplifier
 - Thorlabs M37L02 multimode fiber with a 550- μm core and a 0.22 numerical aperture
 - Edmund Optics integrating sphere
 - Avian Technologies Avian-B barium sulfate white reflectance coating
 - Applied to an aluminum sample holder
 - Optronic Laboratories OL220IR spectral standard lamp
 - Varian Cary 6000i ultraviolet (UV)-visible (Vis)-near infrared (NIR) spectrophotometer
 - 1% ceramic Nd-doped Nd:YAG sample provided by Dr. Larry Merkle
 - 10% crystal Yb-doped Yb:YAG sample borrowed from Dr. Alex Newburgh
-

4. Experiment

The experiment relies upon being able to measure a value for the photon flux in an integrating sphere. An integrating sphere is a hollow sphere made of a highly reflective material such that light in the sphere is scattered evenly throughout. The sphere used in this experiment was one purchased from Edmund Optics. The Spectra-Physics titanium sapphire laser was chopped at 100 Hz and then allowed to shine through one opening of the sphere while a sample holder was positioned at another. Finally, a M37L02 fiber was attached to the sphere so that the light could be guided out of the sphere and into the Fluorolog spectrometer.

In replicating the method of de Mello et al. (1), the integrating sphere was used to capture light from three different scenarios, as shown in figure 1. The first scenario involved only an empty sample holder in the sphere. This was used to measure only the spectrum of the laser line for determining a value of its photon flux, labeled here as L_e to reflect that it is the value for the laser line when the sphere was empty. The second scenario involved the sample being placed in the sphere such that it was not hit by the laser beam directly but was allowed to fluoresce from the scattered laser light. Measuring the photon flux of the fluorescence and the scattered laser beam produced values for F_o and L_o , labeled to reflect that the sample was out of the beam. Finally, the third scenario involved putting the sample directly in the laser beam path and again measuring the photon flux, labeled F_i and L_i for the fact that the sample is in the beam.

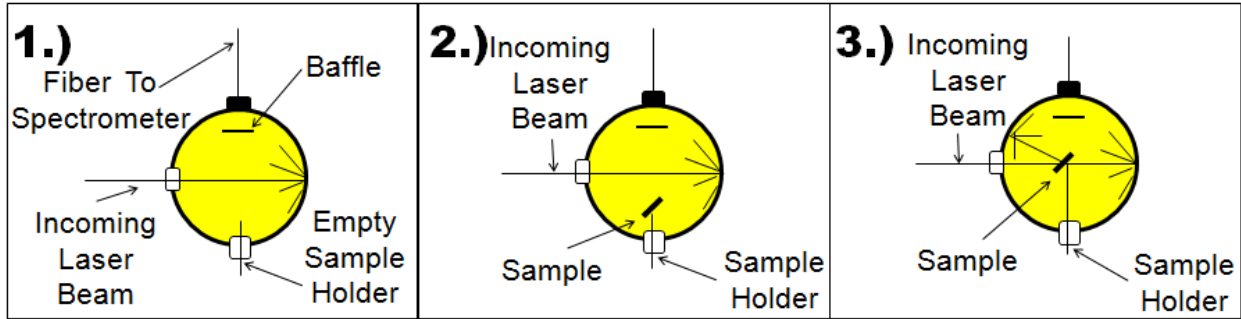


Figure 1. Diagram showing the three scenarios for the quantum efficiency measurement. (1) The sphere is empty. (2) The sample is in the sphere but out of the beam. (3) The sample is in the sphere and in the beam.

With these data, it is possible to determine a value for the quantum efficiency of the material in question using the equation derived by de Mello et al. (1). Through assessing their derivation, their equation for the quantum efficiency, η , was found to be a believable answer when considering a simple model of the integrating sphere system. Therefore, the equation used for this experiment was

$$\eta = \frac{F_i - \left(\frac{L_i}{L_o}\right)F_o}{L_e \left(1 - \frac{L_i}{L_o}\right)} \quad (1)$$

5. Results

In order to validate the experimental method, a reference sample was needed as a standard. The sample would need to be one with a well-known quantum efficiency value and, preferably, limited reabsorption. Because of these requirements, a sample of 1% ceramic Nd:YAG was used due to its well-known quantum efficiency value of close to 1.

During the first attempt at the experiment, a spectrum of the Nd:YAG sample was measured in the three integrating sphere scenarios using the nominally 2.2- μm detector and 1- μm blazed grating. The sample was held in the sphere using a bare aluminum sample holder of unknown reflectivity. The titanium sapphire laser was tuned to a wavelength of 808.6 nm so that the Nd:YAG would be able to absorb the incoming laser light without interfering with the fluorescence. These data were initially inconclusive since a calibration of the sphere and the sensitivity of the InGaAs detector had not been performed. However, it was still believed that it would most likely be incorrect due to the sample holder being made of bare, machined aluminum instead of a material of high reflectivity.

To adjust the data for the system's sensitivity changes at different wavelengths, the OL220IR standard lamp was shone into the integrating sphere in hope of correcting for the system as a whole. The spectrum produced by the integrating sphere system was then divided by the accepted values for the standard lamp's spectrum and normalized. A graph of this system response curve can be found in appendix A. The data set could then be divided by this calibration curve to scale the data relative to the system's highest sensitivity at roughly 1330 nm. Applying this system response curve to the data set and multiplying each data point by its corresponding wavelength to convert to a value of the photon flux in relative units produced the necessary graph for this experiment. When integrated, this graph produced a quantum efficiency value of 0.46.

Since this initial value for the quantum efficiency was far from what was expected, it was decided to first correct the issue of the aluminum holder. To do this, the Avian-B barium sulfate white reflectance coating was purchased and applied to the aluminum holder. Doing this caused the holder to more closely resemble the reflectivity of the integrating sphere. In addition, the nominally 2.2- μm InGaAs detector was replaced with the 2.6- μm detector due to the belief that the longer wavelength detector actually had a slightly higher sensitivity at shorter wavelengths and a higher signal-to-noise ratio. This is reflected when comparing its system response curve to the one previously used. The system response curve for the 2.6- μm detector and 1- μm blazed grating with the coated holder can be found in appendix A.

With these concerns addressed, it was decided to take one more data set for Nd:YAG using the new coated sample holder. Taking this new data set produced the spectrum shown in figure 2 for the case of the sample not in the beam.

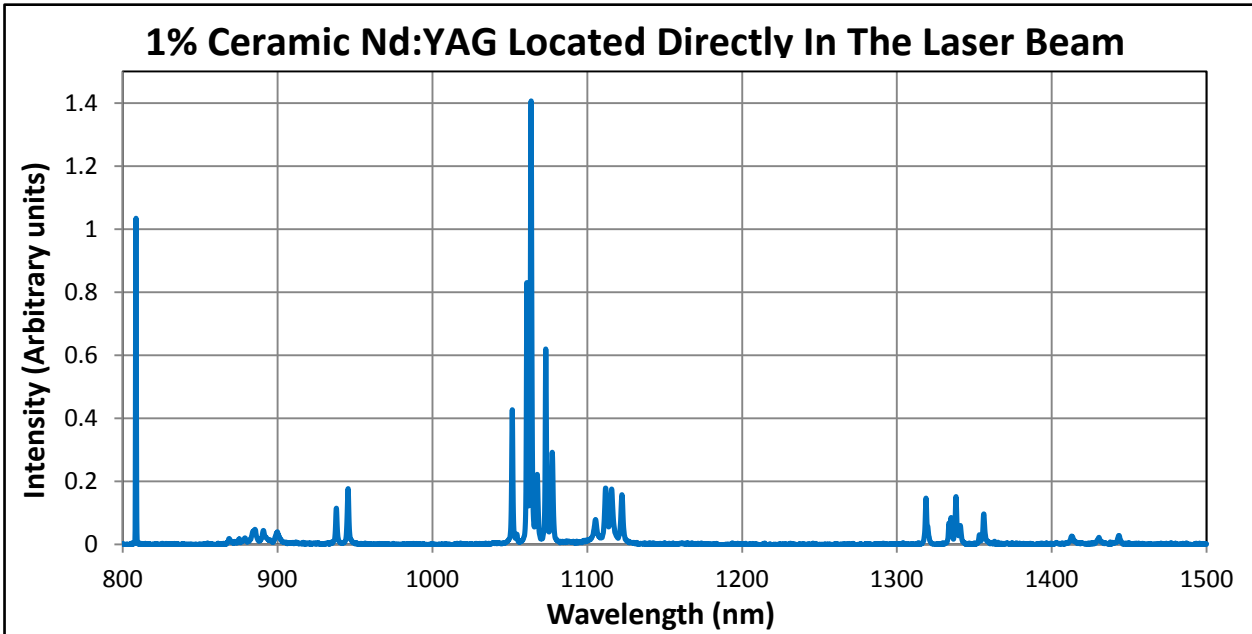


Figure 2. This is the raw spectrum produced by the 1% Nd:YAG sample located directly in the beam. The out of the beam case produced a similar spectrum with smaller fluorescence values and a larger laser line.

Again, these data were corrected by dividing by the appropriate calibration curve. They were then multiplied by wavelength in order to convert from values proportionate to energy to ones proportionate to the photon flux. The process is shown in figure 2 for the out of the beam data set in figure 2. Doing this and then integrating gave the following values for L_e , L_o , L_i , F_o , and F_i (table 1).

Table 1. Values for L_e , L_o , L_i , F_o , and F_i using the 1% Nd:YAG sample.

$L_e = 33376$	$L_o = 29327$	$L_i = 4631$	$F_o = 2047$	$F_i = 15404$
---------------	---------------	--------------	--------------	---------------

For these new data, a quantum efficiency value of 0.54 was obtained. In light of these low results, reabsorption was not considered at this time. In Nd:YAG, reabsorption can occur in the 850-nm region of fluorescence but it should have a small effect on the fluorescence, making it dwarfed by the apparent larger discrepancy. In addition, the calculated branching ratios for the Nd:YAG were within 4% of the accepted values, so it was clear that reabsorption was not impacting the data greatly.

6. Analysis

These results of 0.46 and 0.54, respectively, were obviously much lower than expected for a 1% ceramic Nd:YAG sample and prompted much discussion about possible sources of error. The first thing that was considered was the possibility that the shortest wavelength section of the

system response curve could have an error due to the system's obviously weak detection ability in the region. To test this, it was decided to move further up the curve and excite the Nd:YAG sample at 869 nm. Doing this would avoid some of the system's poorer detection range at the cost of making some of the weaker fluorescence peaks disappear into the laser line. However, doing this produced a result of 0.45 for the quantum efficiency. This was again close to the experiment's previously incorrect answers, shedding no light on the source of the discrepancy.

It was then decided that the concentration of the sample should be checked. This was done by placing the sample in the Cary spectrophotometer and taking a transmission spectrum. Upon doing this, the transmission spectrum was found to agree with accepted values for a 1% ceramic Nd:YAG sample, so a possibility of there being a mislabeling of the concentration was ruled out. The transmission spectrum of the Nd:YAG sample can be found in appendix C.

Finally, a brief experiment was performed to determine the scattering ability of the sphere. To do this, the angle of the incoming beam was changed multiple times and, in a separate experiment, the location of the sample holder was changed multiple times in the case where the sample is not in the beam. The spectra of these measurements allowed us to conclude that the sphere was indeed highly uniform in its scattering as they did not differ significantly.

7. Retrial With 10% Yb:YAG

After considering the difficulties with the 1% Nd:YAG, it was then determined that the experiment should again be performed with a new sample. For this, a sample of 10% Yb:YAG was obtained for its similarly high quantum efficiency. The experiment was repeated by exciting Yb:YAG at 914 nm, with this excitation wavelength chosen in order to interfere with as little of the material's fluorescence as possible. A transmission spectrum of this sample can be found in appendix C. Doing this produced the spectrum in figure 3 for the sample in the beam case. Repeating the previous method of dividing by the system response, multiplying by wavelength, and integrating, these data produced the results in table 2.

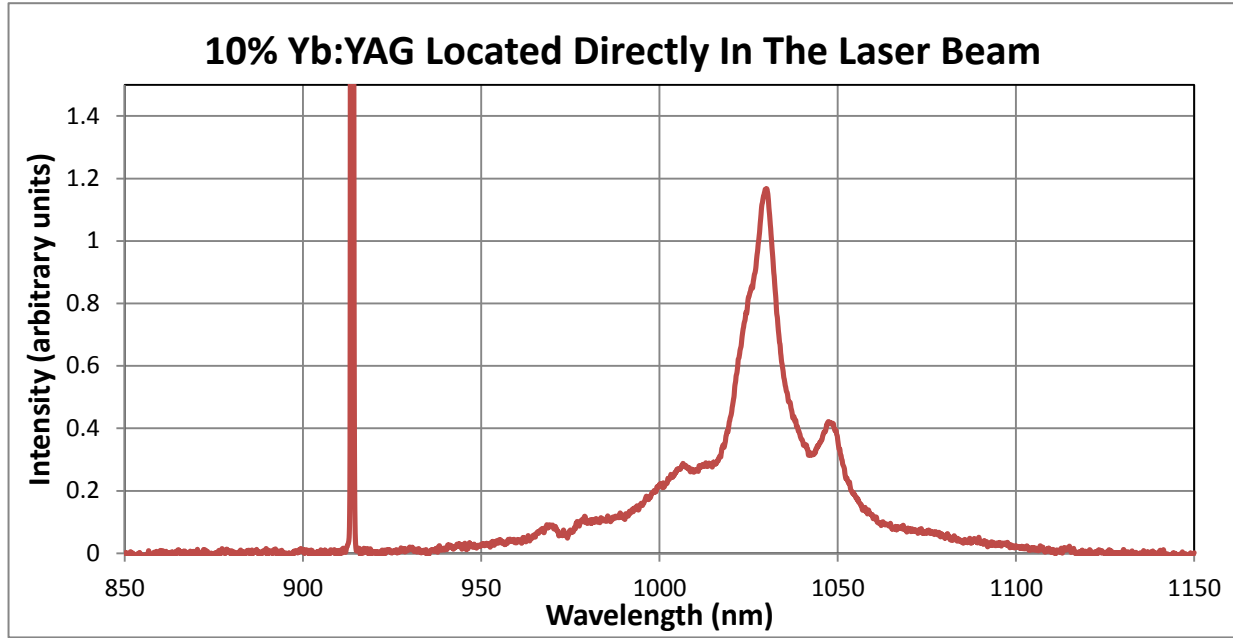


Figure 3. Raw spectrum produced by the 10% Yb:YAG sample located directly in the beam. The out of the beam case produced a similar spectrum with smaller fluorescence values and a larger laser line. The laser line for this scenario peaked at 9.5 on this scale and has been cut off for clarity of the fluorescence spectrum.

Table 2. Values for L_e , L_o , L_i , F_o , and F_i using the 10% Yb:YAG sample.

$L_e = 32087$	$L_o = 29786$	$L_i = 20157$	$F_o = 1416$	$F_i = 11200$
---------------	---------------	---------------	--------------	---------------

In addition, applying the quantum efficiency equation to these data produce a result of 0.98. In contrast to the Nd:YAG sample, this answer agreed with what was expected.

Since the sample was a 10% concentration, reabsorption did indeed have to be reconsidered in this case. To do this, a piece of the sample was cut off and ground into a powder. Then, the powder's spectrum was excited at 914 nm and its spectrum was measured directly by the Fluorolog spectrometer without using the integrating sphere. In addition, the remaining bulk sample also had its spectrum measured directly. Both of these spectra can be found in appendix D. Both sets of data were multiplied by wavelength to convert to photon flux and integrated as described in Ahn et al.'s paper (2) on correcting for a sample's reabsorption. The ratio of the area of the bulk sample's curve to the powder's curve was found and subtracted from 1 to find a value of 0.45 for a , the probability of reabsorption. Then, it was possible to apply their equation

$$\eta_{true} = \frac{\eta_{observed}}{1 - a + a(\eta_{observed})} \quad (2)$$

Their equation was derived by modeling the reabsorption as a geometric series. This method is a reasonable technique for considering the reabsorption and has the added benefit of not being able to produce a value over 1. With this in mind, it adjusted the previously observed quantum efficiency value to a new value of 0.99. It is believable that this reabsorption only made a small

change in the previous result because a high efficiency material would, in theory, lose little light over multiple reabsorption processes since nearly all of the light that is reabsorbed is converted back into fluorescence that would be detected in the integrating sphere.

8. Conclusions

Unfortunately, the problem with this experiment was not solved during this summer's experiments. It was previously thought that the problem had to have been either systematic or theoretical, yet the new results for Yb:YAG have complicated that idea. What remains currently are several possibilities. One of these possibilities is that there is an error in the calibration curve, either in the steep fall off of the systems sensitivity at shorter wavelengths or in our inability to properly calibrate for the fluorescence light originating inside the sphere. This has prompted a presently unfinished critical discussion of the equations used and whether or not they accurately take these factors into account. In addition, the 1% Nd:YAG will most likely be retested using the 940-nm excitation wavelength to further ignore the lowest parts of the detectors sensitivity. Another possibility is that the 1% Nd:YAG ceramic is somehow damaged or defective and thus produces a smaller quantum efficiency value than expected. This is again highly unlikely due to the fact that Nd:YAG is incredibly well studied and this particular sample is believed to be of high quality and to have been stored and handled properly. However, it would explain the results and could possibly be verified by comparing this sample's fluorescence lifetime to accepted values or finding another 1% Nd:YAG sample. These and other possibilities will be tested further by Dr. Larry Merkle.

With this in mind, it is important to note that the experiment still has great potential. Several papers (3, 4) have reported positive results with this method. In addition, it seems to have correctly measured 10% Yb:YAG and has provided fairly precise results, despite yielding most likely inaccurate ones for 1% Nd:YAG. Because of this, the conclusion is that this method still could be an incredibly useful one for finding the quantum efficiency of unknown materials provided that the issues with the previously measured standard samples can be sorted out.

9. References

1. de Mello, J. C.; Wittmann, H. F.; Friend, R. H. *Adv. Materials*. (Weinham Ger) **1997**, *9*, 230.
2. Ahn, T.; Al-Kaysi, R. O.; Muller, A. M.; Wentz, K. M.; Bardeen, C. J. *Rev. Sci. Instrum.* **2007**, *78*, 086105.
3. Porres, L.; Holland, A.; Palsson, L.-O.; Monkman, A. P.; Kemp, C.; Beeby, A. J. *Fluorescence* **2006**, *16* (2), 267.
4. Dong, X.; Du, X.; Liu, Y.; Ren, L.; Jin, L.; Lei, X.; Chen, W. *Proc. SPIE* **2012**, *8560*, 85600O.

INTENTIONALLY LEFT BLANK.

Appendix A. System Response Curves

This first graph (figure A-1) shows the normalized system response curve generated for the aluminum holder in the integrating sphere in conjunction with the 2.2- μm InGaAs detector and the 1- μm blazed grating.

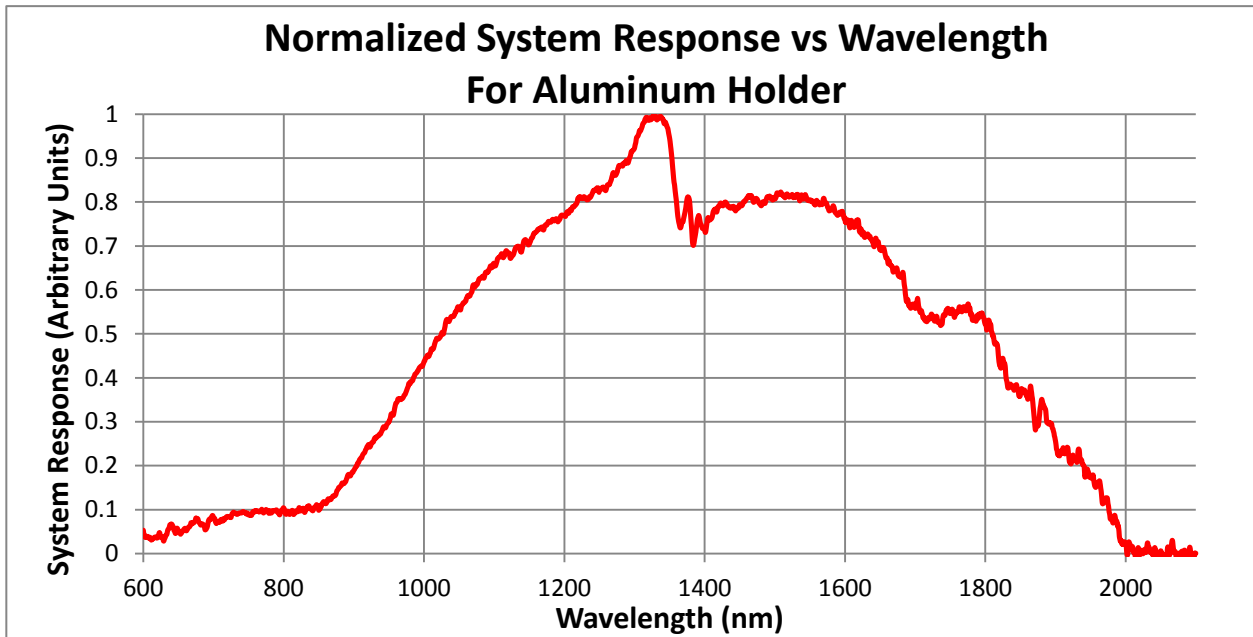


Figure A-1. Normalized system response curve generated for the aluminum holder in the integrating sphere in conjunction with the 2.2- μm InGaAs detector and the 1- μm blazed grating.

This second graph (figure A-2) shows the normalized system response curve obtained when the same method was applied to the coated sample holder in conjunction with the 2.2- μm InGaAs detector and the 1- μm blazed grating.

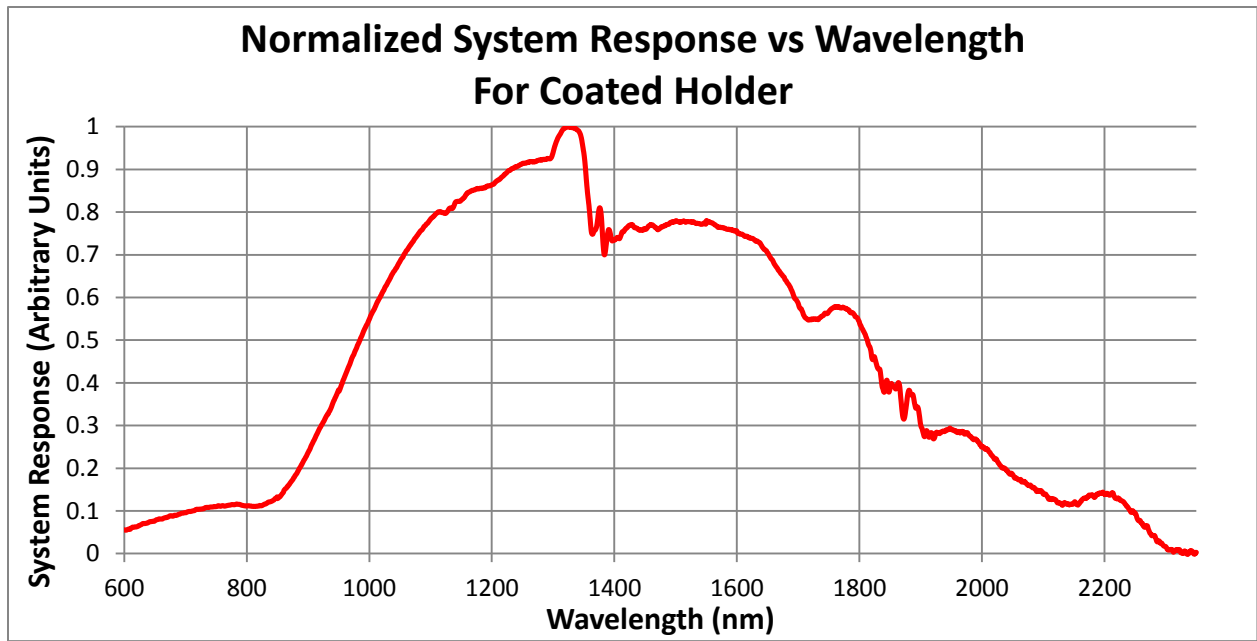


Figure A-2. Normalized system response curve obtained when the same method was applied to the coated sample holder in conjunction with the 2.2- μm InGaAs detector and the 1- μm blazed grating

Appendix B. Example of the Data Analysis

Taking the raw dataset in figure 2 as a starting point, it was then divided by the system response curve to produce a true fluorescence spectrum. This spectrum is shown in figure B-1.

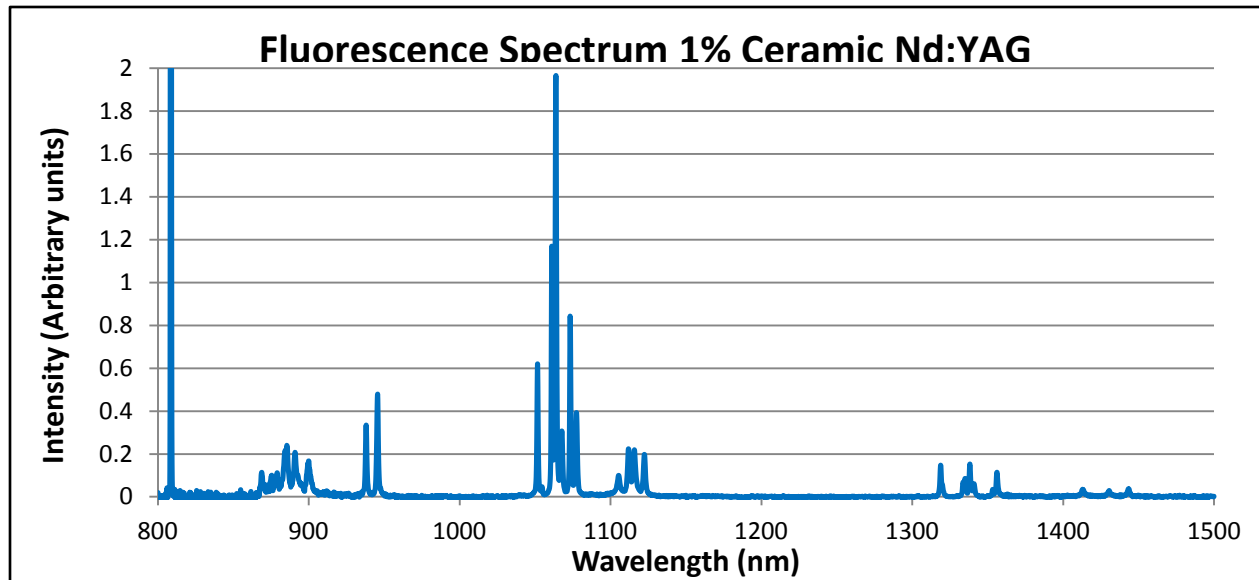


Figure B-1. True fluorescence spectrum of 1% ceramic Nd:YAG.

The laser line at 808.6 nm actually extends to roughly 9.35 on this scale and has been cut off to better show the fluorescence. This true fluorescence spectrum would then be multiplied by wavelength so that the data would become proportionate to the photon flux. Doing this produced the graph in figure B-2.

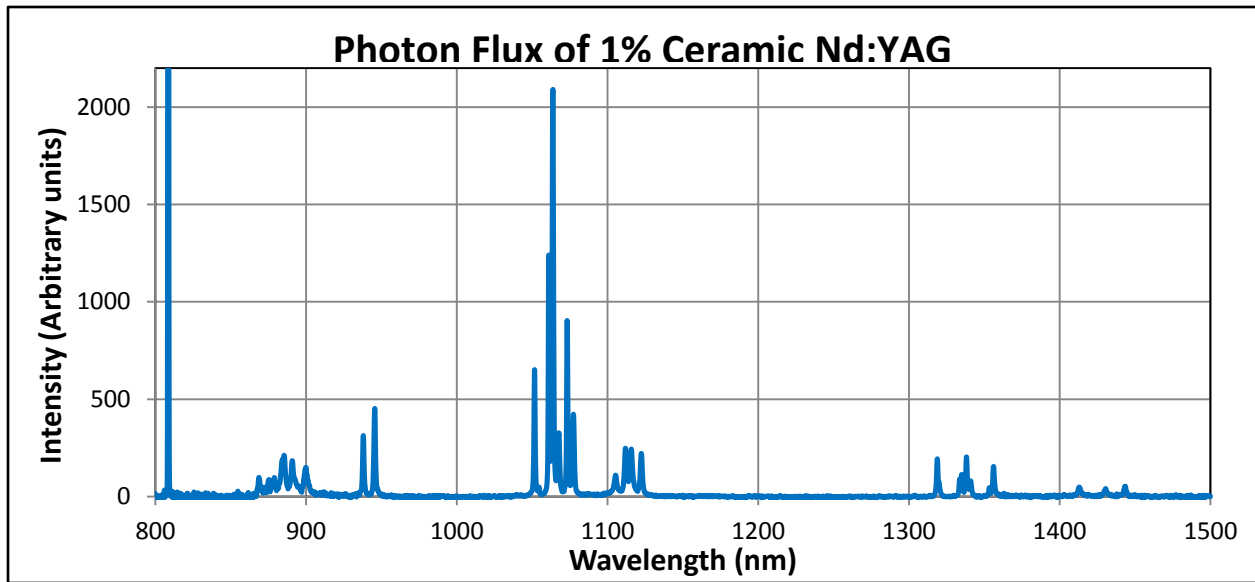


Figure B-2. Photon flux of 1% ceramic Nd:YAG.

Again, the laser line was cut off and really reaches roughly 7500 on this scale. It is this graph that was then integrated to get the necessary values for the quantum efficiency equation.

Appendix C. Transmission Spectra of Samples

This first graph (figure C-1) shows the transmission spectrum for the 1% ceramic Nd:YAG sample used in this experiment.

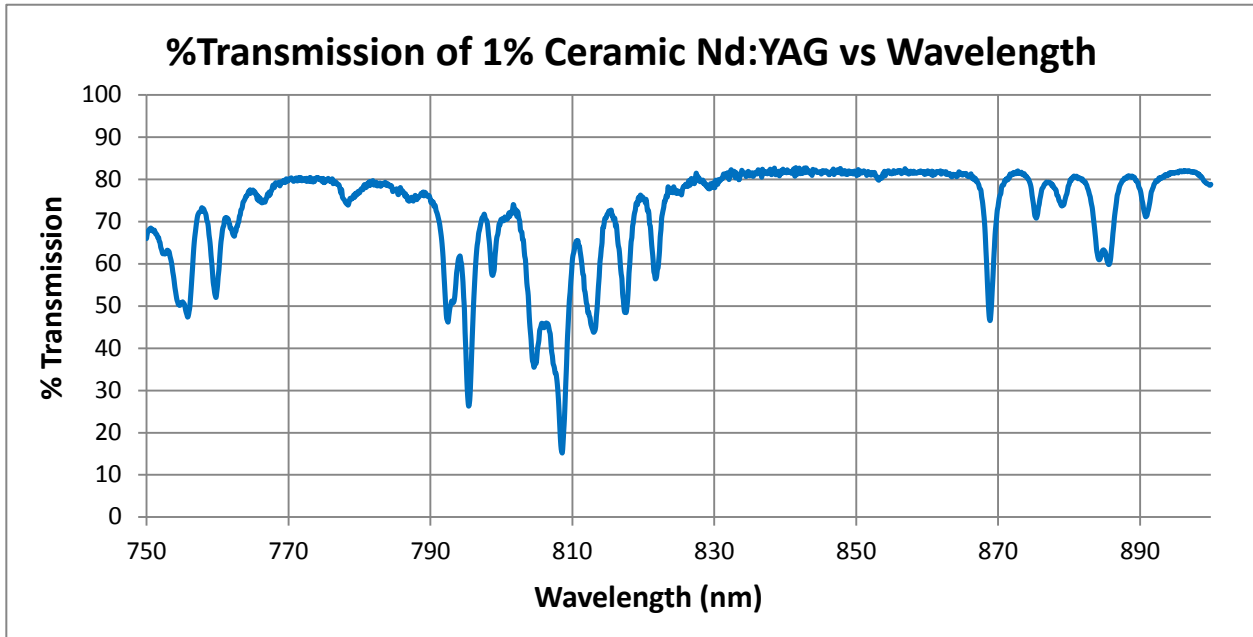


Figure C-1. Transmission spectrum for the 1% ceramic Nd:YAG sample used in this experiment

This second graph (figure C-2) shows the transmission spectrum for the 10% Yb:YAG sample used in this experiment.

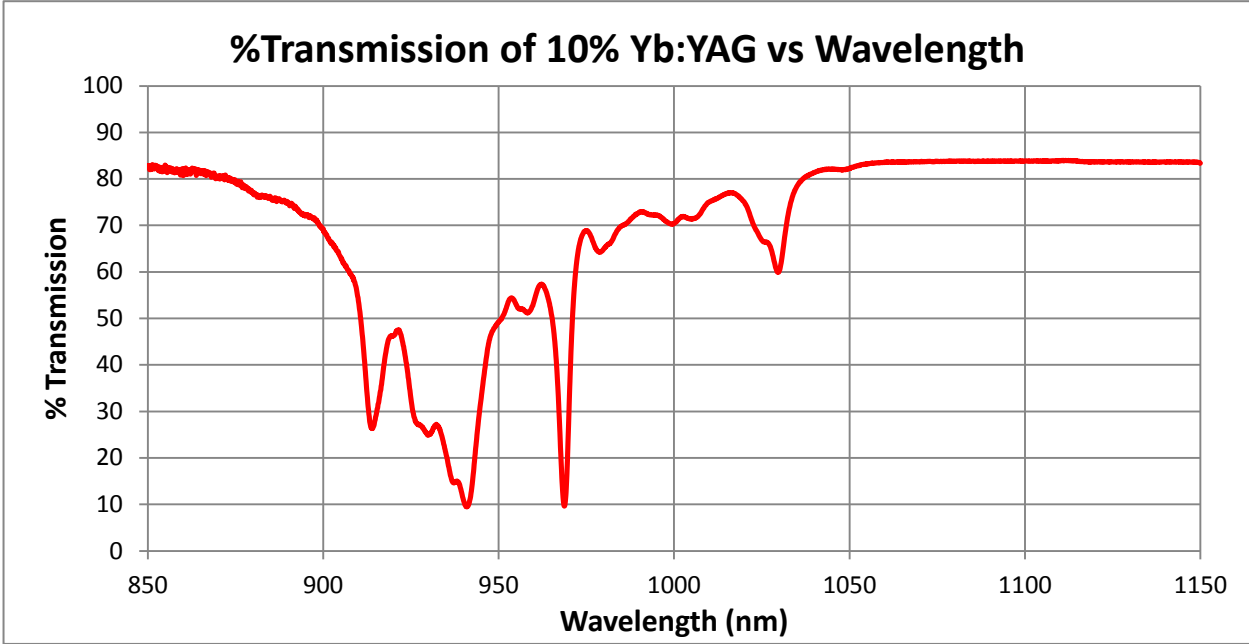


Figure C-2. Transmission spectrum for the 10% Yb:YAG sample used in this experiment.

Appendix D. Data for Reabsorption Determination for Yb:YAG

Figure D-1 shows the graph of the photon flux scaled for the detection system for the powdered sample and the bulk sample measured directly in the spectrometer. The area underneath the bulk curve was divided by the area underneath the powdered curve and subtracted from 1 to calculate the probability of reabsorption.

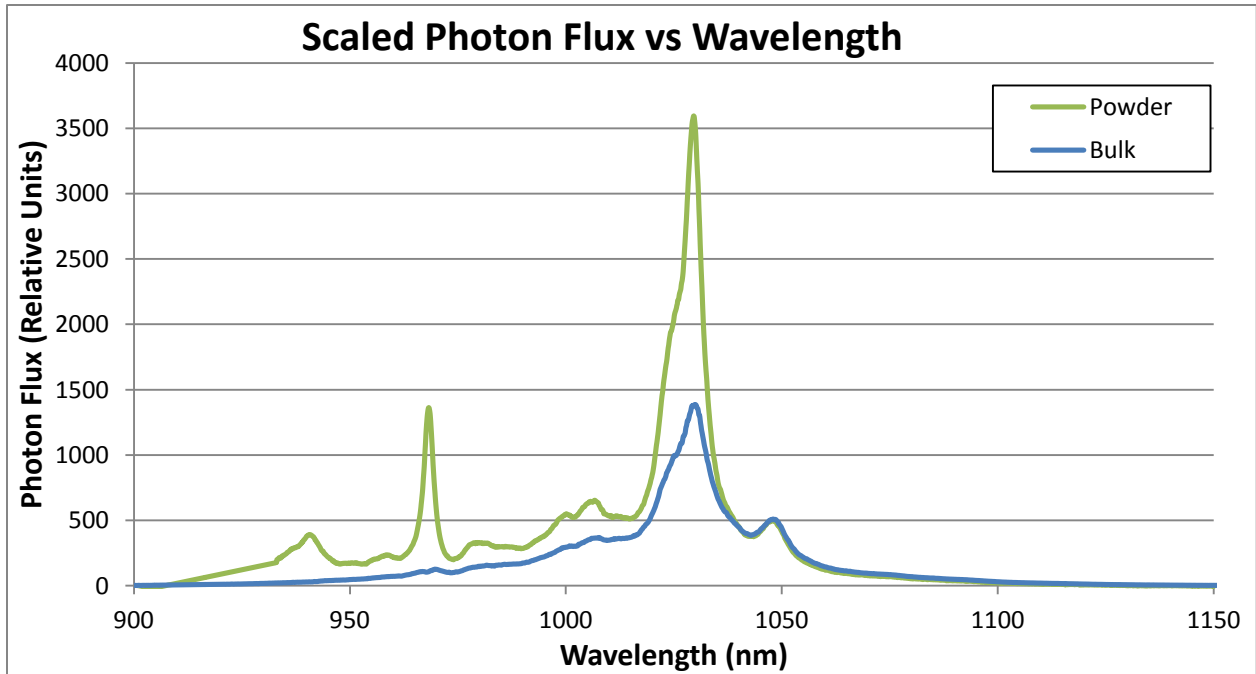


Figure D-1. Photon flux scaled for the detection system for the powdered sample and the bulk sample measured directly in the spectrometer.

1 DEFENSE TECHNICAL
(PDF) INFORMATION CTR
DTIC OCA

2 DIRECTOR
(PDF) US ARMY RESEARCH LAB
RDRL CIO LL
IMAL HRA MAIL & RECORDS MGMT

1 GOVT PRNTG OFC
(PDF) A MALHOTRA

2 DIRECTOR
(PDFS) US ARMY RESEARCH LAB
RDRL SEE M
L MERKLE
S MELIS